Mechanisms of sodium-glucose cotransporter-2 inhibition: Insights from Large-Scale Proteomics

Running title: Proteomics of SGLT2 inhibitors

Ele Ferrannini, MD[1], Ashwin C. Murthy, MD[2], Yong-ho Lee, MD[3], Elza Muscelli, MD[1], Sophie Weiss, PhD[4], Rachel M. Ostroff, PhD[4], Naveed Sattar, MD[5], Stephen A. Williams, PhD[4], Peter Ganz, MD[6]

[1] CNR Institute of Clinical Physiology, Pisa, Italy

[2] Cardiovascular Division, Department of Medicine, Hospital of the University of Pennsylvania, Philadelphia, PA, USA

[3] Department of Medicine, Severance Hospital, Yonsei University College of Medicine, Seoul, South Korea

[4] SomaLogic, Inc., Boulder, CO, USA

[5] Institute of Cardiovascular and Medical Sciences, University of Glasgow, UK

[6] Zuckerberg San Francisco General Hospital, University of California, San Francisco, USA

Corresponding author: Ele Ferrannini, M.D.
CNR Institute of Clinical Physiology
Via Savi, 10 – 56126 Pisa, Italy
Phone: 050-553272
Fax: 050-553235
e-mail: ferranni@ifc.cnr.it

Word count: 2,456
Tables: 2
Figures: 2
Supplemental material: 2 Tables and 2 Figures

Abstract

Objective To assess the effects of empagliflozin, a selective SGLT2 inhibitor, on broad biological systems through proteomics.

Research Design and Methods 3,713 proteins were quantified using aptamer-based proteomics in 144 paired plasma samples obtained from 72 participants across the spectrum of glucose tolerance, before and after 4 weeks of empagliflozin 25 mg/day. Biology of the plasma proteins significantly changed by empagliflozin (at false discovery rate-corrected $p<0.05$) was discerned through Ingenuity Pathway Analysis.

Results Empagliflozin significantly affected levels of 43 proteins, 6 related to cardiomyocyte function (fatty acid binding protein 3 and 4 (FABPA), neurotrophic receptor tyrosine kinase (NTRK2), renin, thrombospondin-4, and leptin receptor), 5 to iron handling (ferritin heavy chain 1, transferrin receptor protein 1 (TFRC), neogenin, growth differentiation factor 2 (GDF-2), and ß2-microglobulin) and 1 to spingosine/ceramide metabolism (neutral ceramidase), a known pathway of cardiovascular disease. Among the protein changes achieving the strongest statistical significance, insulin-like binding factor protein-1 (IGFBP-1), transgelin-2, FABPA, growth differentiation factor-15 (GDF15), and sulphydryl oxidase 2 precursor (QSOX2) were increased, while ferritin, thrombospondin-3, and REarranged during Transfection (RET) were decreased by empagliflozin administration

Conclusion SGLT2 inhibition is associated, directly or indirectly, with multiple biological effects, including changes in markers of cardiomyocyte contraction/relaxation, iron handling, and other metabolic and renal targets. The most significant differences were detected in protein species (GDF15, ferritin, IGFBP-1 and FABP) potentially related to the clinical and metabolic changes that were actually measured in the same patients. These novel results may inform further studies, using targeted proteomics and a prospective design.

Introduction

Sodium-glucose cotransporter-2 (SGLT2) is a transmembrane protein encoded by genes of the *SLC5A* family (1). SGLT2 is a high capacity, low-affinity transporter almost exclusively expressed on the luminal side of the S1 segment of the proximal renal tubule. Its function is to reabsorb glucose and sodium from the glomerular filtrate into the circulation. Convincing evidence shows that SGLT2 is functionally overactive in patients with type 2 diabetes (T2D), in whom it therefore contributes to the hyperglycemia (2,3). SGLT2 inhibition results in urinary excretion of glucose, sodium, and water, leading to hemodynamic changes as well as glycemic improvements in patients with T2D (1). SGLT2 inhibitors (SGLT2i) have been developed as glucose-lowering drugs for the treatment of T2D. Somewhat unexpectedly, large cardiovascular (CV) safety trials testing SGLT2i against placebo in T2D patients at high CV risk have consistently demonstrated clinically relevant benefit for both cardiovascular and renal outcomes (4-6). This has led to changes in clinical recommendations and practice (7,8). As the glucose-lowering efficacy of SGLT2i is generally modest (*i.e.,* HbA_{1c} reductions in the range 0-6-0.8% (9)), it is widely believed that mechanisms other than (or in addition to) glycemic control must be at work to explain the cardiovascular and renal protection of SGLT2i. The recently published DAPA-HF results also suggest that SGLT2i lessen risk of heart failure by mechanisms independent of glycemia since benefits were identical in those with and without diabetes (10). Multiple hypotheses have been advanced, not necessarily exclusive of one another. Thus, SGLT2i-induced natriuresis and osmotic diuresis with blood volume contraction may be responsible for the reduction in blood pressure and arterial stiffness, which can improve cardiac function by decreasing both pre- and afterload (11,12). Also, SGLT2i may optimize tissue energy metabolism and mitochondrial bioenergetics in impaired heart and kidney by supplying an excess of 'thrifty' substrates (*e.g.,* ketones) (13). Reduction of uricemia

(14), modulation of the tubulo-glomerular feedback (15), and lowering of inflammation and fibrosis biomarkers (16) are additional putative contributors to reported benefits.

From the *in vivo* mechanistic information so far gathered, it is likely that the primary action of SGLT2i on the proximal renal tubule induces a range of physiological consequences in several domains of bodily functions. Proteomics is a useful approach to explore canonical biological pathways in a hypothesis-free fashion (17). This prompted us to screen the plasma proteome of individuals with T2D or impaired glucose tolerance (IGT) receiving SGLT2i treatment by applying a large-scale version of an aptamer-based multiplex proteomics platform (SOMAscan) to quantify plasma proteins (18).

Methods

Study population A total of seventy-two participants (25 women and 47 men) were recruited into the study (**Table S1**). Of these, 61 were patients with T2D (29 were drug-naïve or off any glucose-lowering agent for at least 12 weeks, and 32 were on a stable dose of metformin of $\geq 1{,}500$ mg/day for at least 12 weeks). Inclusion criteria were either sex, age >18 years, body mass index (BMI) 20–40 kg/m^2, HbA$_{1c}$ 6.5–10.5% (48-91 mmol/mol), and estimated glomerular filtration rate (eGFR) >60 ml$^.$min$^{-1.}$1.73m^{-2} (by the CKD-EPI equation (19)). Duration of diabetes was <1 year in 3%, <5 years in 18%, <10 years in 26%, and ≥ 10 years in 19% of the patients. Exclusion criteria were: history of malignancy in the last 5 years; significant cardiovascular disorder within last 6 months; pregnancy or women expecting to conceive within the study duration; bariatric surgery within the past 2 years; treatment with antiobesity drugs in the last 3 months; neurogenic bladder disorders; ALT and AST >3.0 *x* ULN; changes in thyroid hormone dosage within 6 weeks or any other endocrine disease except T2D; alcohol or drug abuse. Detailed metabolic analysis of these

patients has been published previously (20). Eleven subjects with IGT (by ADA criteria) were included; their anthropometric and metabolic characteristics have been reported (21).

Protocol One hundred and fourty-four fasting EDTA plasma samples were obtained from the participants at baseline and after 4 weeks of treatment with 25 mg/day empagliflozin. The modified aptamer binding reagents, SomaScan assay and its performance characteristics have previously been described (22-25). In brief, each of the individual proteins measured has its binding reagent made of chemically modified DNA, referred to as a modified aptamer. Each plasma sample was incubated with the mixture of modified aptamers to generate modified aptamer-protein complexes under equilibrium conditions. Unbound modified aptamers and unbound or nonspecifically bound proteins were eliminated by 2 bead-based immobilization steps. After elution of the modified aptamers from the target protein, the fluorescently labeled modified aptamers were directly quantified on hybridization array (Agilent Technologies). Calibrators were included so that the degree of fluorescence was a consistent reflection of protein concentration. Protein concentration was expressed as relative fluorence units (RFU). All samples were placed randomly on 96-well plates, run in a single batch, and normalized against protein calibrator samples included on each plate. Technicians were blinded to the before and after status of samples. Details of scaling, normalization and control of batch effects are given in (26). Median intra- and interassay coefficients of variation are ~5% (25). A total of 4,005 proteins were measured, 292 of them failed to pass SomaLogic's quality control metrics, leaving 3,713 proteins for analysis. Differences between the baseline and 4-week samples were expressed as $\log_2$ ratios for each of the proteins measured.

Plasma glucose and creatinine concentrations were measured by standard laboratory methods. Creatinine clearance was measured on carefully collected urine samples as the ratio of urinary creatinine excretion and plasma creatinine levels.

Statistical analysis Differences between on-treatment and baseline values were analyzed by the Wilcoxon signed-rank test for paired comparisons in 3,713 protein measurements; *p* values were corrected for multiple comparisons using both the Bonferroni family-wise error rate correction and the Benjamini-Hochberg false discovery rate (FDR) correction. Proteins with an FDR-adjusted value of *p*<0.05 were considered statistically significant for inclusion in the pathway analysis. Ingenuity Pathway Analysis (IPA) was used to cluster differentially expressed proteins after 4 weeks of treatment compared with baseline into pathways and functional groups. For those modified aptamers that had multiple Uniprot identifications associated with one result, only the first listed Uniprot identification was used in pathway analysis (27). The Fisher right-tailed exact test was used to calculate a *p* value to determine the probability that the association of the differently expressed proteins in the measured data set and the pathway is explained by chance alone. Correction for changes in creatinine clearance was carried out using a mixed model with patient ID as a random effect.

Results

As expected, in the whole group of subjects 4 weeks of treatment resulted in significant decreases of body weight and body, HbA$_{1c}$, fasting glycemia and creatinine clearance (Supplemental Table S1).

Of the 3,713 proteins measured, 21 were not recognized by IPA, and the remainder were used as background reference. No statistically significant differences in the within-subject responses were seen between baseline and treatment in the 3 groups of participants (drug-naïve T2D, metformin-treated T2D, and IGT) ($r^2 = 0.035$, *p*=0.22). There were also no discernible differences on an individual protein target level, as evidenced by univariate Kruskal-Wallis tests, on the within-subject (baseline minus treatment) differences (*e.g.,* **Figure 1**). Therefore, in all subsequent

analyses the three groups were treated as one.

On an initial screen using an FDR p value ≤ 0.05 corrected for 3,713 dimensions, 44 proteins were associated with a significant change between baseline and treatment (16 reaching a Bonferroni p value<0.05) (**Table 1**). Pathway analysis grouped these proteins into biological pathways ranging from iron handling and cardiomyocyte contractility and relaxation to lipid and glucose metabolism (**Figure 2**). The target proteins – and their genes – that showed the largest change with treatment (*i.e.,* a percent change lower than -15% or higher than +19%) with an FDR $p<0.05$ (model 1) are listed in **Table 2**.

Creatinine clearance was mildly but significantly reduced after 4 weeks of empagliflozin treatment (Table 1). This change may bias the assessment of treatment effects because of accumulation of waste products in the blood. The analysis was therefore repeated after adjustment for individual changes in creatinine clearance (model 2). Several proteins that were significant (at the FDR $p<0.05$ level) in model 1 lost significance. In particular, seven protein targets with p values <0.05 moved to p values >0.20 after the correction for creatinine clearance: cystatin-SN (CST1.5459.33.3), guanylate cyclase activator 2B (uroguanylin, GUCA2B.6223.5.3), trefoil factor 3 (TFF3.4721.54.2), C-C motif chemokine 15 (CCL15.3509.1.1), thrombospondin-4 (THBS4.3340.53.1), renin (REN.3396.54.2), and neutral ceramidase (ASAH2.3212.30.3).

The results of model 2 are given in **Table S2** in descending order of FDR corrected p values, down to a p value <0.10.

Discussion

Empagliflozin treatment for 4 weeks altered the proteomic profile in the plasma of individuals with T2D. Among the proteins that changed in response to treatment, pathway analysis indicated that their biological roles pertained to lipid and glucose metabolism, iron handling, cardiomyocyte

function (contraction and relaxation), cytokines, and molecular transport. In accord with previous metabolic results in these subjects (21,28), there was no formally tested difference across background antihyperglycemic treatment (metformin or none) or glucose tolerance status (T2D *vs* IGT). This made it possible to analyze all available data as one set.

Circulating protein concentrations are the net balance of release into the bloodstream (resulting from changes in gene expression/transcription and/or cellular secretion/shedding) and removal from the plasma (by degradation or excretion). Empagliflozin, like other SGLT2i, causes a reduction in eGFR, which persists as long as treatment continues and is reversed on stopping it (4,9,14). eGFR adjustment of our patients' proteomic profile was therefore necessary to protect against bias introduced by hemodynamic and filtration changes. It is of interest that with eGFR adjustment 7 proteins lost strength of association with treatment. Among them is cystatin, a clinical marker of GFR, and 3 other proteins – renin, guanylate cyclase activator 2B, and trefoil factor 3 – that also are influenced by changes in GFR. This finding, along with the use of nonparametric testing and stringent multicomparison *p*-value restriction, adds confidence in the reliability of the remaining observed treatment-induced protein changes.

Among the plasma protein changes achieving the strongest statistical significance, IGFBP-1, transgelin-2, FABPA, GDF15, and QSOX2 were increased by empagliflozin, while ferritin, thrombospondin-3, and RET were decreased. Interpretation of the biological significance of such changes in the context of the biochemical modifications observed *in vivo* must be done with caution. In fact, ingenuity pathway analysis almost invariably suggests that any given protein plots on to several different pathways. Thus, IGFBP-1 – produced mainly by the liver in response to nutritional stimuli – acts as a transport protein of IGF to prolong its half-life, guide a tissue-specific localization, and modulate its actions (29) (**Figure S1**). A strong, consistent association between circulating IGFBP-1 and insulin sensitivity has been reported in diverse populations (30).

Furthermore, plasma IGFBP-1 levels are inversely correlated with leptin levels (31). In T2D

patients, SGLT2i treatment reduces visceral fat (32) and ameliorates insulin resistance (20,33,34).

This may suggest a causal path whereby empagliflozin improves insulin resistance through

upregulation of IGFBP-1. However, IGFBP-1 is also involved in RXR activation and estrogen

receptor signaling (33), vascular function (35), cell migration *via* integrin (36), and pancreatic ß-cell

regeneration (37). Therefore, additional links to IGFBP-1 may emerge as the range of physiological

consequences of SGLT2 therapy in patients with diabetes is expanded and physiologically

explained.

Serum ferritin, a key parameter of iron homeostasis (**Figure S2**), also is a well-known marker

reflecting insulin resistance and liver fat accumulation (38). The reduced ferritin levels after

empagliflozin (-34%) resonate with the alleviation of hepatic steatosis reported in several studies of

SGLT2i (39,40). On the other hand, the reduction in ferritin may be linked with the observed (mild

and transient) increase in erythropoietin (21), reflecting a boost in erythropoiesis (41).

GDF15, a member of the transforming growth factor-β (TGF-β) superfamily, is a myomitokine

whose induction in mice protects against the onset of obesity and insulin resistance by promoting

oxidative function and lipolysis in liver and adipose tissue (42). GDF15 has recently received

interest as a potential therapeutic target in obesity as well as cancer-associated cachexia (43).

Recently, glial-cell-derived neurotrophic factor receptor α-like (GFRAL) was identified as a specific

receptor of GDF15, requiring the co-receptor RET to execute intracellular signaling (44,45). In the

current data, the joint increase in GDF15 and decrease in RET (Table 3) might stand for a

coordinated stress-like response to empagliflozin-induced weight loss (41), and/or such changes

may contribute to the weight loss associated with SGLT2i therapy. As a general tissue stress and

injury signal, GDF15 has been reported to be a predictive biomarker for cardiovascular events and

death in individuals with dysglycemia (42). It is intriguing that in the large cardiovascular

outcomes trial, ORIGIN, GDF15 was found to be increased in patients with T2D on treatment with metformin (48).

Fatty acid-binding protein 4 (FABP4) is primarily located in adipocytes and macrophages (49). It has been implicated in the pathogenesis of insulin resistance and atherosclerosis (50). FABP4 is released from adipocytes in a non-classical pathway associated with lipolysis. In the patients in the present study, empagliflozin stimulated lipolysis through a reduction in plasma insulin concentrations (20). The observed increase in plasma FABP4 can therefore be plausibly connected with an increased lipolysis.

The thrombospondin family consists of adhesive glycoproteins that mediate cell-to-cell and cell-to-matrix interactions (51). Thrombospondin-3, which is abundant in muscle and kidney, is linked to the endoplasmic reticulum (ER) stress response (52). Presumably, abatement of ER stress by SGLT2 inhibition may relate to the 16% decrement in thrombospondin-3 levels found in the present study.

This exploratory study has limitations. The sample size was modest, with no placebo control, and treatment only lasted 4 weeks. We therefore opted for a conservative analysis of the proteomic data so as to down-rank random variation between baseline and treatment. That noted, we did see the expected changes in glycemia, weight and eGFR, and in surrogates of liver fat, lending external validity to the findings. We cannot exclude the possibility that the proteome might change further with prolonged treatment, nor can we extrapolate the findings in our cohort of well-controlled patients free of macro- and microvascular complications to the participants of the EMPAREG OUTCOME trial (4), who had established cardiovascular disease. While vascular and/or renal complications are likely to add their specific proteomic signatures, the protein panel here described may reflect early effects of SGLT2 inhibition.

In conclusion, treatment with empagliflozin in patients with T2D was associated with a shift in the plasma proteome. The most significant differences were detected in protein species potentially related to the clinical and metabolic changes that were actually measured in the same patients (20). Novel results on GDF15, ferritin, IGFBP-1 and FABP should stimulate further studies, using targeted proteomics and a prospective design. At present, our findings represent the first hypothesis-free evidence that SGLT2 inhibition affects the plasma proteome in a biologically plausible fashion.

Acknowlegments

The authors thank the SomaLogic assay team and Darryl Perry for the bioinformatics.

Author Contributions

E.M., S.W., and R.M.O. researched data. S.A.W. and P.G. reviewed/edited the manuscript. Y-H.L., A.C.M., N.S. contributed to the discussion and reviewed/edited the manuscript. E.F. conceived the study and wrote the manuscript.

References

1. Ferrannini E. Sodium-Glucose Co-transporters and Their Inhibition: Clinical Physiology. Cell Metab 2017; 26:27-38.
2. Norton L, Shannon CE, Fourcaudot M, Hu C, Wang N, Ren W, Song J, Abdul-Ghani M, DeFronzo RA, Ren J, Jia W. Sodium-glucose co-transporter (SGLT) and glucose transporter (GLUT) expression in the kidney of type 2 diabetic subjects. Diabetes Obes Metab 2017;19:1322-1326.
3. Solini A, Rossi C, Mazzanti CM, Proietti A, Koepsell H, Ferrannini E. Sodium-glucose co-transporter (SGLT)2 and SGLT1 renal expression in patients with type 2 diabetes. Diabetes Obes Metab 2017;19:1289-1294.
4. Zinman B, Wanner C, Lachin JM, Fitchett D, Bluhmki E, Hantel S, Mattheus M, Devins T, Johansen OE, Woerle HJ, Broedl UC, Inzucchi SE; EMPA-REG OUTCOME Investigators. Empagliflozin, Cardiovascular Outcomes, and Mortality in Type 2 Diabetes. N Engl J Med 2015;373:2117-2128.
5. Neal B, Perkovic V, Mahaffey KW, de Zeeuw D, Fulcher G, Erondu N, Shaw W, Law G, Desai M, Matthews DR; CANVAS Program Collaborative Group. Canagliflozin and Cardiovascular and Renal Events in Type 2 Diabetes. N Engl J Med 2017;377:644-657.
6. Wiviott SD, Raz I, Bonaca MP, Mosenzon O, et al.; DECLARE–TIMI 58 Investigators. Dapagliflozin and Cardiovascular Outcomes in Type 2 Diabetes. N Engl J Med 2019;380:347-357.
7. Professional Practice Committee: Standards of Medical Care in Diabetes-2019. Diabetes Care 2019;42(Suppl 1):S3.
8. Cosentino F, Grant PJ, Aboyans V, et al. 2019 ESC Guidelines on diabetes, pre-diabetes, and cardiovascular diseases developed in collaboration with the EASDD. Eur Heart J 2020;41:255-323.
9. Kramer CK, Zinman B. Sodium-Glucose Cotransporter-2 (SGLT-2) inhibitors and the Treatment of Type 2 Diabetes. Ann Rev Med 2019;70:323-34.
10. McMurray JJV, Solomon SD, Inzucchi SE, et al.: DAPA-HF Trial Committees and Investigators. Dapagliflozin in Patients with Heart Failure and Reduced Ejection Fraction. NEJM 2019;381:1995-2008.
11. Verma S, McMurray JJV. SGLT2 inhibitors and mechanisms of cardiovascular benefit: a state-of-the-art review. Diabetologia 2018;61:2108-2117.
12. Zelniker TA, Braunwald E. Cardiac and Renal Effects of Sodium-Glucose Co-Transporter 2 Inhibitors in Diabetes: JACC State-of-the-Art Review. J Am Coll Cardiol 2018;72:1845-1855.
13. Ferrannini E, Mark M, Mayoux E. CV Protection in the EMPA-REG OUTCOME Trial: A "Thrifty Substrate" Hypothesis. Diabetes Care 2016;39:1108-14.
14. DeFronzo RA, Norton L, Abdul-Ghani M. Renal, metabolic and cardiovascular considerations of SGLT2 inhibition. Nat Rev Nephrol 2017;13:11-26.
15. Cherney DZ, Perkins BA, Soleymanlou N, Maione M, Lai V, Lee A, Fagan NM, Woerle HJ, Johansen OE, Broedl UC, von Eynatten M. Renal hemodynamic effect of sodium-glucose cotransporter 2 inhibition in patients with type 1 diabetes mellitus. Circulation 2014;129: 587-597.

16. Heerspink HJL, Perco P, Mulder S, Leierer J, Hansen MK, Heinzel A, Mayer G. Canagliflozin reduces inflammation and fibrosis biomarkers: a potential mechanism of action for beneficial effects of SGLT2 inhibitors in diabetic kidney disease. Diabetologia 2019;62:1154-66.
17. Lindsey ML, Mayr M, Gomes AV, Delles C, Arrell DK, Murphy AM, Lange RA, Costello CE, Jin YF, Laskowitz DT, Sam F, Terzic A, Van Eyk J, Srinivas PR; American Heart Association Council on Functional Genomics and Translational Biology, Council on Cardiovascular Disease in the Young, Council on Clinical Cardiology, Council on Cardiovascular and Stroke Nursing, Council on Hypertension, and Stroke Council. Transformative Impact of Proteomics on Cardiovascular Health and Disease: A Scientific Statement From the American Heart Association. Circulation 2015;132:852–872.
18. Ganz P, Heidecker B, Hveem K, Jonasson C, Kato S, Segal MR, Sterling DG, Williams SA. Development and Validation of a Protein-Based Risk Score for Cardiovascular Outcomes Among Patients With Stable Coronary Heart Disease. JAMA 2016;315:2532–2341.
19. Levey AS, Stevens LA. Estimating GFR using the CKD Epidemiology Collaboration (CKD-EPI) creatinine equation: more accurate GFR estimates, lower CKD prevalence estimates, and better risk predictions. Am J Kidney Dis 2010;55: 622-627.
20. Ferrannini E, Muscelli E, Frascerra S, Baldi S, Mari A, Heise T, Broedl UC, Woerle HJ. Metabolic response to sodium-glucose cotransporter 2 inhibition in type 2 diabetic patients. J Clin Invest 2014;124:499-508.
21. Ferrannini E, Baldi S, Frascerra S, Astiarraga B, Heise T, Bizzotto R, Mari A, Pieber TR, Muscelli E. Shift to Fatty Substrate Utilization in Response to Sodium-Glucose Cotransporter 2 Inhibition in Subjects Without Diabetes and Patients With Type 2 Diabetes. Diabetes 2016;65:1190-1195.
22. Rohloff JC, Gelinas AD, Jarvis TC, Ochsner UA, Schneider DJ, Gold L, Janjic N. Nucleic acid ligands with protein-like side chains: modified aptamers and their use as diagnostic and therapeutic agents. Mol Ther Nucleic Acids 2014;3, e201.
23. Gold L, Ayers D, Bertino J, et al. Aptamer-based multiplexed proteomic technology for biomarker discovery. PLoS ONE 2010; 5, e15004.
24. Kim CH, Tworoger SS, Stampfer MJ, Dillon ST, Gu X, Sawyer SJ, Chan AT, Libermann TA, Eliassen AH. Stability and reproducibility of proteomic profiles measured with an aptamer-based platform. Sci Rep 2018; 8, 8382.
25. Candia J, Cheung F, Kotliarov Y, Fantoni G, Sellers B, Griesman T, Huang J, Stuccio S, Zingone A, Ryan BM, Tsang JS, Biancotto A. Assessment of variability in the SOMAscan assay. Sci Rep 2017; 7, 14248.
26. Williams SA, Kivimaki M, Langenberg C, et al. Plasma Protein patterns as comprehensive indicators of health. Nature Med 2019;25:1851-1857.
27. Williams SA, Murthy AC, DeLisle RK, Hyde C, Malarstig A, Ostroff R, Weiss SJ, Segal MR, Ganz P. Improving Assessment of Drug Safety Through Proteomics: Early Detection and Mechanistic Characterization of the Unforeseen Harmful Effects of Torcetrapib. Circulation 2018;137:999-1010.
28. Muscelli E, Astiarraga B, Barsotti E, Mari A, Schliess F, Nosek L, Heise T, Broedl UC, Woerle HJ, Ferrannini E. Metabolic consequences of acute and chronic empagliflozin administration in treatment-naive and metformin pretreated patients with type 2 diabetes. Diabetologia 2016;59:700-708.
29. Haywood NJ, Slater TA, Matthews CJ, Wheatcroft SB. The insulin like growth factor and binding protein family: Novel therapeutic targets in obesity & diabetes. Mol Metab 2019;19:86-96.

30. Abbas A, Grant PJ, Kearney MT. Role of IGF-1 in glucose regulation and cardiovascular disease. Expert Rev Cardiovasc Ther 2008;6:1135-49.
31. Söderberg S, Ahrén B, Eliasson M, Dinesen B, Brismar K, Olsson T. Circulating IGF binding protein-1 is inversely associated with leptin in non-obese men and obese postmenopausal women. Eur J Endocrinol 2001;144:283-290.
32. Bolinder J, Ljunggren Ö, Kullberg J, Johansson L, Wilding J, Langkilde AM, Sugg J, Parikh S. Effects of dapagliflozin on body weight, total fat mass, and regional adipose tissue distribution in patients with type 2 diabetes mellitus with inadequate glycemic control on metformin. J Clin Endocrinol Metab 2012;97:1020-31.
33. Kotronen A, Lewitt M, Hall K, Brismar K, Yki-Järvinen H. Insulin-like growth factor binding protein 1 as a novel specific marker of hepatic insulin sensitivity. J Clin Endocrinol Metab 2008;93:4867–4872.
34. Merovci A, Solis-Herrera C, Daniele G, Eldor R, Fiorentino TV, Tripathy D, Xiong J, Perez Z, Norton L, Abdul-Ghani MA, DeFronzo RA. Dapagliflozin improves muscle insulin sensitivity but enhances endogenous glucose production. J Clin Invest. 2014;124:509-14.
35. Rajwani A, Ezzat V, Smith J, et al. Increasing circulating IGFBP1 levels improves insulin sensitivity, promotes nitric oxide production, lowers blood pressure, and protects against atherosclerosis. Diabetes 2012;61:915–924.
36. Jones JI, Gockerman A, Busby WH Jr, Wright G, Clemmons DR. Insulin-like growth factor binding protein 1 stimulates cell migration and binds to the alpha 5 beta 1 integrin by means of its Arg-Gly-Asp sequence. Proc Natl Acad Sci U S A 1993;90:10553–10557.
37. Lu J, Liu K-C, Schulz N, Karampelias C, Charbord J, Hilding A, Rautio L, Bertolino P, Östenson C-G, Brismar K, Andersson O. IGFBP1 increases β-cell regeneration by promoting α- to β-cell transdifferentiation. EMBO J 2016;35:2026-44.
38. Fernandez-Real JM, Ricart-Engel W, Arroyo E, Balançá R, Casamitjana-Abella R, Cabrero D, Fernández-Castañer M, Soler J. Serum ferritin as a component of the insulin resistance syndrome. Diabetes Care 1998;21:62-68.
39. Sattar, N., Fitchett D, Hantel S, George JT, Zinman B. Empagliflozin is associated with improvements in liver enzymes potentially consistent with reductions in liver fat: results from randomised trials including the EMPA-REG OUTCOME(R) trial. Diabetologia 2018;61:2155-2163.
40. Shibuya, T., Fushimi N, Kawai M, Yoshida Y, Hachiya H, Ito S, Kawai H, Ohashi N, Mori A. Luseogliflozin improves liver fat deposition compared to metformin in type 2 diabetes patients with non-alcoholic fatty liver disease: A prospective randomized controlled pilot study. Diabetes Obes Metab 2018;20:438-442.
41. Eschbach JW, Haley NR, Egrie JC, Adamson JW. A comparison of the responses to recombinant human erythropoietin in normal and uremic subjects. Kidney Int 1992;42:407-16.
42. Chung HK, Ryu D, Kim KS, et al. Growth differentiation factor 15 is a myomitokine governing systemic energy homeostasis. J Cell Biol 2017;216:149-165.
43. Tsai VWW, Husaini Y, Sainsbury A, Brown DA, Breit SN. The MIC-1/GDF15-GFRAL Pathway in Energy Homeostasis: Implications for Obesity, Cachexia, and Other Associated Diseases. Cell Metab 2018;28:353-368.
44. Yang L, Chang CC, Sun Z, et al. GFRAL is the receptor for GDF15 and is required for the anti-obesity effects of the ligand. Nat Med 2017;23:1158-1166.
45. Hsu JY, Crawley S, Chen M, et al. Non-homeostatic body weight regulation through a brainstem-restricted receptor for GDF15. Nature 2017;550:255-259.

46. Ferrannini G, Hach T, Crowe S, Sanghvi A, Hall KD, Ferrannini E. Energy Balance After Sodium-Glucose Cotransporter 2 Inhibition. Diabetes Care 2015;38:1730-1735.

47. Gerstein HC, Paré G, McQueen MJ, Haenel H, Lee SF, Pogue J, Maggioni AP, Yusuf S, Hess S; Outcome Reduction With Initial Glargine Intervention Trial Investigators. Identifying Novel Biomarkers for Cardiovascular Events or Death in People With Dysglycemia. Circulation 2015;132:2297-2304.

48. Gerstein HC, Pare G, Hess S, Ford RJ, Sjaarda J, Raman K, McQueen M, Lee S, Haenel H, Steinberg GR; ORIGIN Investigators. Growth Differentiation Factor 15 as a Novel Biomarker for Metformin. Diabetes Care 2017;40:280-283.

49. Hotamisligil GS, Bernlohr DA. Metabolic functions of FABPs--mechanisms and therapeutic implications. Nat Rev Endocrinol 2015;11:592-605.

50. Furuhashi M. Fatty Acid-Binding Protein 4 in Cardiovascular and Metabolic Diseases. J Atheroscler Thromb 2019;26:216-232.

51. Adolph KW, Long GL, Winfield S, Ginns EI, Bornstein P. Structure and organization of the human thrombospondin 3 gene (THBS3). Genomics 1995;27:329-336.

52. Schips TG, Vanhoutte D, Vo A, Correll RN, Brody MJ, Khalil H, Karch J, Tjondrokoesoemo A, Sargent MA, Maillet M, Ross RS, Molkentin JD. Thrombospondin-3 augments injury-induced cardiomyopathy by intracellular integrin inhibition and sarcolemmal instability. Nat Commun 2019;10:76.doi: 10.1038/s41467-018-08026-8.

Table 1 – Top protein targets with an FDR *p* value <0.05.

Target	Entrez Gene	UniProt	log₂ fold-change	*p* value	Bonferroni *p*	FDR
IGFBP-1	*IGFBP1*	P08833	0.53	2.57E-11	9.54E-08	6.72E-08
Ferritin	*FTH1 FTL*	P02794 P02792	-0.60	3.62E-11	1.34E-07	6.72E-08
DSC2	*DSC2*	Q02487	0.11	2.32E-08	8.62E-05	1.78E-05
FABPA	*FABP4*	P15090	0.30	2.39E-08	8.90E-05	1.78E-05
FABP	*FABP3*	P05413	0.23	4.00E-08	0.00015	2.48E-05
HE4	*WFDC2*	Q14508	0.14	7.50E-08	0.00028	3.98E-05
TSP3	*THBS3*	P49746	-0.26	3.64E-07	0.0014	0.00016
TFF3	*TFF3*	Q07654	0.12	3.86E-07	0.0014	0.00016
MIC-1	*GDF15*	Q99988	0.27	5.33E-07	0.0020	0.00020
QSOX2	*QSOX2*	Q6ZRP7	0.26	2.15E-06	0.0080	0.00073
TMEDA	*TMED10*	P49755	0.14	3.71E-06	0.014	0.0011
Renin	*REN*	P00797	0.20	4.14E-06	0.015	0.0011
FAM3B	*FAM3B*	P58499	0.13	4.61E-06	0.017	0.0011
TR	*TFRC*	P02786	0.17	4.99E-06	0.019	0.0012
MRC2	*MRC2*	Q9UBG0	-0.19	5.86E-06	0.022	0.0013
MIP-5	*CCL15*	Q16663	0.11	9.53E-06	0.035	0.0020
BSP	*IBSP*	P21815	0.20	2.35E-05	0.088	0.0042
NEO1	*NEO1*	Q92859	-0.11	2.35E-05	0.088	0.0042
Leptin R	*LEPR*	P48357	0.09	3.13E-05	0.12	0.0052
PTPRU	*PTPRU*	Q92729	-0.17	3.25E-05	0.12	0.0052
Trypsin	*PRSS1*	P07477	0.15	8.26E-05	0.31	0.013
IL-1 sRII	*IL1R2*	P27930	-0.09	0.00011	0.42	0.016
ITIH3	*ITIH3*	Q06033	0.10	0.00011	0.42	0.016
CYTN	*CST1*	P01037	0.13	0.00016	0.58	0.022
OMD	*OMD*	Q99983	-0.16	0.00016	0.61	0.022
MINP1	*MINPP1*	Q9UNW1	0.09	0.00017	0.63	0.022
PAPP-A	*PAPPA*	Q13219	0.16	0.00019	0.71	0.024
RNAS6	*RNASE6*	Q93091	0.13	0.00022	0.82	0.026
SECTM1	*SECTM1*	Q8WVN6	0.15	0.00024	0.87	0.027
GDF2	*GDF2*	Q9UK05	-0.19	0.00024	0.89	0.027
CYTT	*CST2*	P09228	0.09	0.00025	0.91	0.027
ß2-Microglobulin	*B2M*	P61769	0.13	0.00025	0.93	0.027
RNAS4	*RNASE4*	P34096	0.07	0.00027	1	0.028
Transgelin-2	*TAGLN2*	P37802	0.55	0.00035	1	0.035
CBLN4	*CBLN4*	Q9NTU7	-0.12	0.00035	1	0.035
CD59	*CD59*	P13987	0.08	0.00036	1	0.035
ASAH2	*ASAH2*	Q9NR71	-0.16	0.00038	1	0.035
TSP4	*THBS4*	P35443	-0.23	0.00041	1	0.037
Collectin Kidney 1	*COLEC11*	Q9BWP8	-0.10	0.00043	1	0.037
Afamin	*AFM*	P43652	-0.10	0.00043	1	0.037
SIAT9	*ST3GAL5*	Q9UNP4	0.12	0.00050	1	0.042
RET	*RET*	P07949	-0.29	0.00052	1	0.043
TrkB	*NTRK2*	Q16620	-0.11	0.00056	1	0.046

Table 2 – Protein targets with a log$_2$ fold-change absolute value >0.25 (*i.e.*, % change lower than -15% or higher +19%) and an FDR *p*<0.05.

Target	Gene	% change	*p*	Bonferroni *p*	FDR
IGFBP-1	*IGFBP1*	+44	2.57E-11	6.72E-08	9.54E-8
Ferritin	*FTH1*	-34	3.62E-11	6.72E-08	1.34E-07
FABPA	*FABP4*	+23	2.39E-08	1.78E-05	8.90E-05
Thrombospondin-3	*THBS3*	-16	3.64E-07	0.00016	0.0014
GDF15	*GDF15*	+21	5.33E-07	0.00020	0.0020
QSOX2	*QSOX2*	+20	2.15E-06	0.00073	0.0080
Transgelin-2	*TAGLN2*	+46	0.00035	0.035	1
RET	*RET*	-18	0.00052	0.043	1

Table S1 – Anthropometric and metabolic characteristics of the study subjects.*

	Baseline	4 weeks	*p*
Age (years)	60 ± 9	-	-
Body weight (kg)	96 ± 16	94 ± 16	<0.0001
Body mass index (kg·m^{-2})	31.6 ± 4.6	31.1 ± 4.5	<0.0001
HbA$_{1c}$ (%)	7.2 ± 1.0	6.8 ± 0.8	<0.0001
Fasting plasma glucose (mmol/L)	7.5 ± 1.6	6.4 ± 1.0	<0.0001
Creatinine clearance (ml·min^{-1}·1.73m^{-2})	101 ± 24	97 ± 24	0.0023

*entries are mean ± SD; *p* values are from Wilcoxon

Table S2 – Protein targets with an FDR *p*<0.10 adjusted for creatinine clearance.

TARGET	Gene	UniProt	*p*	Bonferroni *p*	FDR
Ferritin	*FTH1 FTL*	P02794 P02792	1.44E-12	5.35E-09	5.22E-09
IGFBP-1	*IGFBP1*	P08833	2.81E-12	1.04E-08	5.22E-09
FABPA	*FABP4*	P15090	1.46E-06	0.0054	0.0012
FABP	*FABP3*	P05413	1.66E-06	0.0062	0.0012
HE4	*WFDC2*	Q14508	2.03E-05	0.075	0.013
BSP	*IBSP*	P21815	2.65E-05	0.098	0.014
MIC-1	*GDF15*	Q99988	3.81E-05	0.14	0.018
QSOX2	*QSOX2*	Q6ZRP7	4.99E-05	0.19	0.021
TR	*TFRC*	P02786	5.78E-05	0.22	0.021
PTPRU	*PTPRU*	Q92729	0.00011	0.42	0.038
FAM3B	*FAM3B*	P58499	0.00012	0.46	0.038
TMEDA	*TMED10*	P49755	0.00018	0.65	0.047
TFF3	*TFF3*	Q07654	0.00018	0.65	0.047
GDF2	*GDF2*	Q9UK05	0.00025	0.93	0.062
S22AG	*SLC22A16*	Q86VW1	0.00028	1	0.064
DSC2	*DSC2*	Q02487	0.00040	1	0.087
SLIK3	*SLITRK3*	O94933	0.00048	1	0.099

Figure 1 – Boxplots of values (as $\log_{10}$ RFU) of 6 target proteins in subjects with impaired glucose tolerance (IGT), drug-naïve type 2 diabetes (T2D), or metformin-treated type 2 diabetes (T2D$_m$) before (*b*) and after (*a*) treatment with empagliflozin.
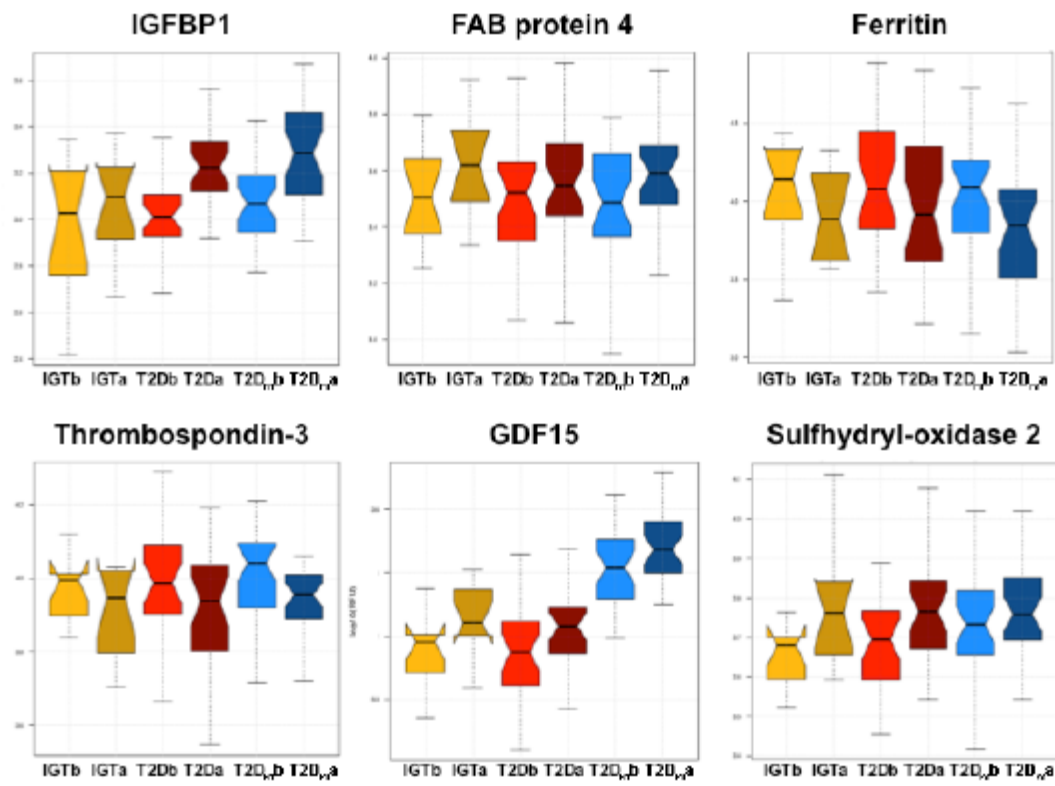
Iron Handling	FDR *p* value
Transferrin receptor protein 1 (TFRC)	0.00116
Beta-2 microglobulin (B2M)	0.0266
Ferritin heavy chain (FTH1)	6.72E-08
Neogenin (NEO1)	0.00417
Growth differentiation factor 2 (GDF2)	0.0266

Cardiomyocyte contraction or relaxation	FDR *p* value
Desmocollin 2 (DSC2)	1.78E-05
Fatty acid binding protein 4 (FABP4)	1.78E-05
Fatty acid binding protein 3 (FABP3)	2.48E-05
Renin (REN)	0.0011
Leptin Receptor (LEPR)	0.00525
Thrombospondin 4 (THBS4)	0.0371
Neurotrophic receptor tyrosine kinase 2 (NTRK2)	0.0456

Lipid & Glucose Metabolism	FRD *p* value
Insulin-like growth factor-binding protein 1 (IGFBP1)	6.72E-08
Fatty acid binding protein 4 (FABP 4)	1.78E-05
Fatty acid binding protein 3 (FABP 3)	2.48E-05
Growth differentiation factor 15 (GDF-15)	0.000198
Renin (REN)	0.0011
Leptin Receptor (LEPR)	0.00525
Pappalysin-1 (PAPPA)	0.0238
Beta 2 microglobulin (B2M)	0.0266
CD59 glycoprotein (CD59)	0.0345
Lactosylceramide alpha-2;3-sialyltransferase (ST3GAL5)	0.042
Neogenin (NEO1)	0.00417
Interleukin-1 receptor type 2 (IL1R2)	0.0163
Neurotrophic receptor tyrosine kinase 2 (NTRK2)	0.0456

↑
↓

Genitourinary Effects	FDR *p* value
Insulin-like growth factor-binding protein 1 (IGFBP1)	6.72E-08
Fatty acid binding protein 4 (FABP4)	1.78E-05
WAP four-disulfide core domain 2 (WFDC2)	3.98E-05
Trefoil factor 3 (TFF3)	0.000159
Growth differentiation factor 15 (GDF-15)	0.000198
Renin (REN)	0.0011
Family with sequence similarity 3 member B (FAM3B)	0.00114
Transferrin receptor protein 1 (TFRC)	0.00116
C-C motif chemokine ligand 15 (CCL15)	0.00197
Integrin binding sialoprotein (IBSP)	0.00417
Leptin Receptor (LEPR)	0.00525
Cystatin-SN (CST1)	0.0216
Pappalysin-1 (PAPPA)	0.0238
Beta 2 microglobulin (B2M)	0.0266
Secreted and transmembrane protein 1 (SECTM1)	0.0266
Ribonuclease 4 (RNASE4)	0.0282
Lactosylceramide alpha-2;3-sialyltransferase (ST3GAL5)	0.042
Ferritin heavy chain (FTH1)	6.72E-08
Thrombospondin 3 (THBS3)	0.000159
Neogenin (NEO1)	0.00417
Receptor-type tyrosine-protein phosphatase U (PTPRU)	0.00525
Osteomodulin (OMD)	0.0216
Growth differentiation factor 2 (GDF2)	0.0266
Cerebellin 4 (CBLN4)	0.0345
Afamin (AFM)	0.0371
Collectin subfamily member 11 (COLEC11)	0.0371
Thrombospondin 4 (THBS4)	0.0371
Ret proto-oncogene (RET)	0.0429
Neurotrophic receptor tyrosine kinase 2 (NTRK2)	0.0456

Figure 2 – Distribution of the top 56 treatment-induced proteins into biological categories by pathway analysis.

Figure S1 – **Network centered on IGFBP-1 of proteins significantly altered by empagliflozin.**
Nodes represent gene symbol name, corresponding to protein measured. The degree of intensity of
the node color (red) indicates degree of significance of *p*-value. Nodes not colored are proteins
either not significant or not measured. The lines correspond to the implicated function of the given
proteins according to the IPA knowledge bank. The node shapes denote enzyme (◊), transporter (▱
), growth factor (▱), transmembrane receptor (⊙), peptidase (◇), phosphatase (△), kinase (▽),
transcription regulator (◯), translation regulator (◇), ion channel (▯), cytokine (▢), chemical (◯
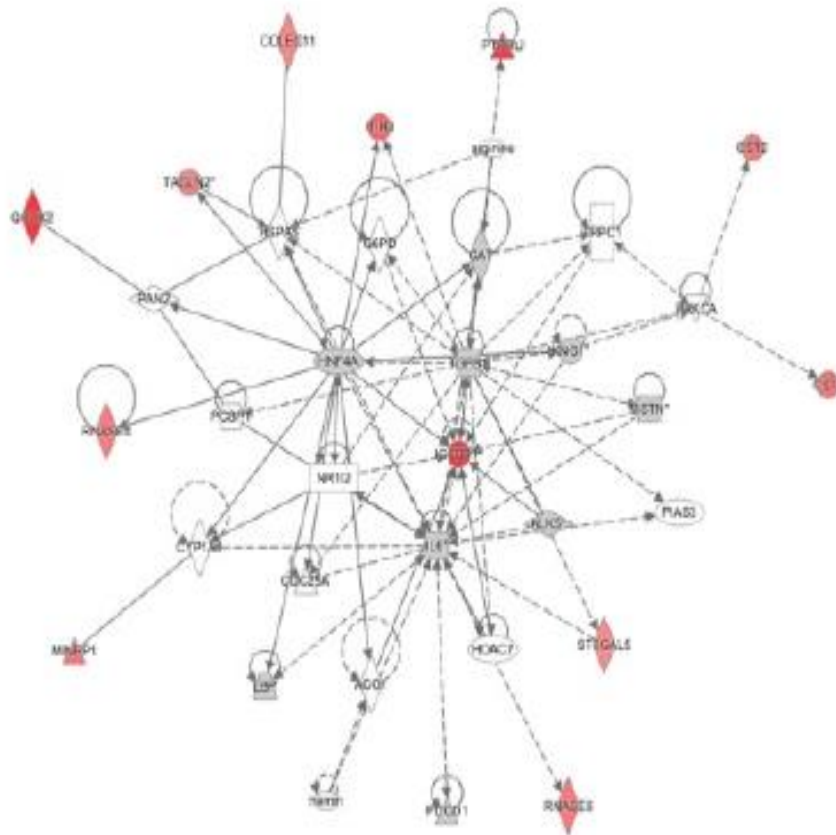), ligand dependent nuclear receptor (▭) and other (◯).

Figure S2 – **Proteins significantly altered by empagliflozin associated with iron homeostasis.**
Nodes represent gene symbol name, corresponding to protein measured. The degree of intensity of
the node color (red) indicates degree of significance of *p*-value. The dashed lines correspond to the
implicated function of the given proteins according to the IPA knowledge bank. The node shapes
denote cytokine (□), transmembrane receptor (○), transporter (□), transcription regulator (○), and
enzyme (◇).